AUTONOMOUS LAND VEHICLE GUIDANCE FOR NAVIGATION IN BUILDINGS BY COMPUTER VISION, RADIO, AND PHOTOELECTRIC SENSING TECHNIQUES

Yih-Ming Su and Wen-Hsiang Tsai*

Institute of Computer and Information Science
National Chiao Tung University
Hsinchu, Taiwan 30050, R.O.C.

Key Words: autonomous land vehicle, vision-based guidance, collision avoidance, corridor navigation, elevator entering.

ABSTRACT

An integrated approach to vision-based autonomous land vehicle (ALV) guidance for automatic navigation and collision avoidance in building corridors and elevators is proposed. Computer vision techniques are utilized to locate an ALV in building corridors and to control it to enter elevators by the use of multiple corner points on walls. The location principle is based on matching input corner position information with a model using a distance-weighted correlation function. Furthermore, radio equipment is employed to control the elevator operations of lifting up, lifting down, door closing, and door opening so that the ALV can enter elevators automatically. Finally, a photoelectric sensor-based obstacle avoidance system for the ALV is developed. A real ALV was constructed as a testbed. Many successful navigation experiments confirm the effectiveness of the proposed approach.

用電腦視覺、無線通訊及光電感應技術作室內自動車航行導引

蘇義明　蔡文祥*

國立交通大學資訊科學系

摘　要

本文提出一個利用電腦視覺讓自動車可以在建築物走廊及電梯中自動航行及避碰的整合方法。首先我們利用電腦視覺技術及牆上眾多角點來定出自動車在走廊中的位置，並控制它進入電梯。定位的原理是把輸入的角點資訊與模式

*Correspondence addressee

作比對，來算出一個以位置作加權的相關函數值。另外，我們利用一個無線電裝置來控制電梯的上下及開關，以便自動車能自動進出電梯。最後，我們利用光電感應器，發展出一套避碰的方法。我們亦建造了一輛真實的自動車來作實驗之用。很多成功的航行試驗證明本文所提方法之有效性。

INTRODUCTION

Vision-based guidance of the autonomous land vehicle (ALV) is based on the use of visual cameras and computer vision techniques. It is a more flexible and intelligent ALV guidance method, and the most similar to the human vision function. Furthermore, vision-based guidance of the ALV has great application potential. A goal of this research is to accomplish automatic guidance of the ALV in indoor environments by integrating computer vision and other sensing techniques using house corner information. Another goal is to develop an ALV which can be used to transport a person from one location to another automatically.

A lot of approaches have been proposed for ALV guidance in indoor environments [1-7]. Blanche [3] is an experimental autonomous vehicle designed by the AT&T Bell Laboratory for indoor navigation. Only two sensors are employed by Blanche. One is an odometer to estimate positions and orientations, and the other is an infrared range finder to provide the vehicle with the 2-D maps of its environment. Accumulated odometer errors are removed by reading barcodes which are mounted around the environment as global beacons. Madarasz et al. [7] designed an autonomous wheelchair which navigates by path planning, corridor following, and obstacle detection and avoidance. An ultrasonic range finder is used to detect obstacles and the dead-ends of corridors, and a camera is used for corridor following and room label recognition. Chatila and Laumond [1] proposed the idea of map generation and vehicle location by map matching in a building. Object vertices were proposed for use as the main features in their matching procedure.

In Ke and Tsai [6], a corner tracking approach was proposed, in which corners in the building are stored as the model, and a method for rotating the camera to track corners was proposed. The idea is to select visible right-angle corners in indoor environments as guiding marks. In Cheng and Tsai [2], a model matching guidance approach was proposed. The locations of vertical lines in indoor environments are used as the model. The vertical line position information is matched with the model to locate the ALV accurately. The distance weighted correlation (DWC) measure is used for model matching. The speed of navigation is about 20 cm/sec.

Although many guidance approaches have been developed for ALV navigation, little research has been conducted on automatic between-floor transportation in buildings. Several problems in addition to the conventional corridor navigation problem must be solved to make between-floor transportation practical. These problems include: (1) remote control of elevator operations like lifting up, lifting down, door opening, door closing; (2) automatic door entering and exit; (3) automatic wall detection, etc. A desirable between-floors ALV system must be able to locate itself accurately without requiring a change in environments or without being influenced by environments. It should also be functional both in corridors and in elevators. Model matching is a reasonable approach for use in such a system. Selecting stable features and developing effective methods to extract these features are the keys to success for this model-based approach. In this study, corners are selected for guidance in corridors and elevators because corners are abundant and easily visible in buildings, and are convenient for use as reference models. Such corners include the intersection points of baselines and vertical lines on the wall; baseline ends; door, window, or elevator corners; etc. Some such corners are shown in Fig. 1. The global position of each corner is measured in advance by hand for use in the model.

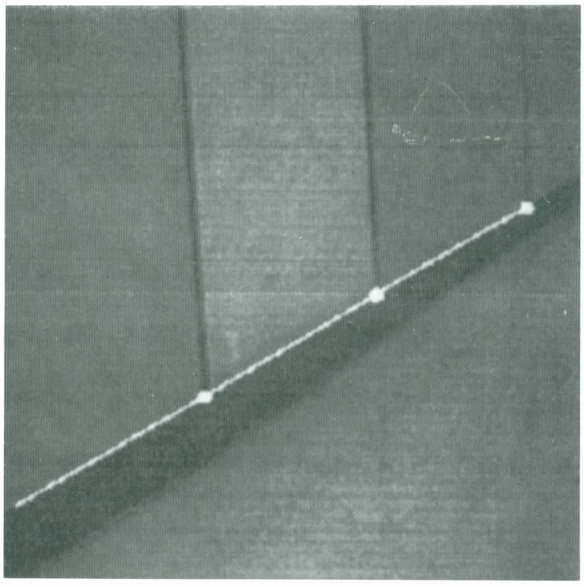

Fig. 1. Example of multiple corners found in a building corridor.

It is necessary to control a standard elevator remotely if automatic transportation between floors is to be fully accomplished. Radio equipment has been designed in this study to control elevator operations by programmable commands. Besides this, an automatic elevator entering system has also been developed. It is based on the same guidance approach as that for corridor navigation, except that an additional camera is employed to obtain images inside the elevator.

For collision avoidance during ALV navigation sessions, several photoelectric sensors are utilized to detect obstacles. Acting in combination, these sensors provide sufficient data to operate a real-time collision avoidance scheme which can detect and avoid unknown static or moving obstacles in building corridors and elevators. If an obstacle (an object or the elevator door) is encountered during an ALV navigation session, the ALV will stop and wait for the obstacle to move away, or will perform the elevator entering process.

A prototype ALV as shown in Fig. 2 is constructed as a testbed for this study. It is a commercial motor-driven vehicle which has been modified by adding sensors, electronic controls, an on-board microcomputer, and several power conversion devices. It has four wheels. The front two are the turning wheels and the rear two are the driving wheels. The front wheels can be controlled to turn leftward or rightward as desired. The rear wheels can be controlled to go forward or backward. A cross-shaped rack on which three CCD cameras and three photoelectric sensors are mounted is located above the front wheels. A microcomputer with a central processor PC486 is located under the footboard. And a battery set providing power to the system is placed under the chair.

Fig. 2. The new prototype ALV used in this study.

The rear part of the ALV includes a motor controller, a motor driver, and a DC-to-DC converter set. All processing tasks for path following, obstacle detection and avoidance, and motion control are performed by the microcomputer.

In our experiments, we use two of the vehicle's three cameras. The cameras have a resolution of 512 × 486 picture elements. The lower camera is used to obtain the image of the baseline of the wall in building corridors, and the upper camera is to obtain the image of the baseline of the wall inside the elevator. Of the three photoelectric sensors used to detect obstacles, the right one is used to detect the elevator door at an intermediate distance, the upper to detect the front space of the ALV at a longer distance, and the third to detect the elevator wall at a shorter distance.

This concludes section 1. Section 2 describes the principle of the ALV navigation techniques proposed. Section 3 describes the ALV location technique employed in this study. Section 4 includes a description of the experimental results. Conclusions and suggestions for future research are found in the final section.

PRINCIPLE OF ALV NAVIGATION

An ALV should be able to determine its current position in each navigation cycle, and plan a path through the environment from its current position to the location of the goal. To perform such functions, the navigation system must be able to identify a variety of visual features. The visual features must aid the ALV in locating itself relative to its surroundings. Also, of course, the objective of ALV navigation is to keep the ALV as close to the desired path as possible. In this study, corners in indoor environments are used as visual features, and the desired path is set up by the user before navigation. Photoelectric sensors are used to detect obstacles. This reduces image processing complexity. In the following, navigation in different environments will be discussed in two sections.

1. Corridor navigation process

In the proposed approach, a navigation session proceeds in a cycle by cycle manner. The ALV location at image taking in a navigation cycle is obtained via a matching process against the model. At the start of a cycle, an image is obtained by the lower camera. After image processing and inverse perspective transformation have been performed, the baseline segments and the corners in the image are extracted, and their positions are transformed into global coordinates. These corners are represented by a point set in a 2-D space, neglecting the height coordinates. So, the matching problem can be regarded as a 2-D point set matching problem. A matching scheme using the distance-weighted correlation

(DWC) function [6] as the match measure is employed. Through the matching procedure, the ALV can be located accurately. But the ALV moves forward for a certain distance during the time interval from obtaining the image to completing the calculation of the ALV position. Thus the computed ALV position must be modified. The details will be described later. After the real ALV position is obtained, the slope of the baseline segment is computed and used to determine the orientation of the ALV. After the position and orientation of the ALV are determined, a control strategy [2] is employed to drive the ALV as close as possible to a given path. This strategy involves adjusting the direction of the driving wheel to ensure safe and smooth ALV navigation. In a straight corridor, the desired path is the center line of each corridor section. In a turning area, multiple line segments are used to approximate a curved path through the area.

2. Elevator entering process

In the elevator entering process, the ALV not only has to perform model-based navigation, but also has to control elevator operations. For the former problem, the model matching process using corners as described in the last section is also employed. Various reference corners can be found inside the elevator. The upper camera is employed to obtain images during the elevator entering process. When the ALV comes close to the elevator door, it will detect the existence of the door. After the door is open, it will execute the ALV navigation cycle as if it was in a building corridor.

The role played by the radio equipment specially designed for this study is to act as an interface between the central processor PC486 and the elevator. Each operation request is issued by the central processor PC486 to the transmitter part of the radio equipment. The receiver part of the radio equipment, which is installed in the top of the elevator room, receives request signals through radio communication and sends corresponding signals to the elevator interface. The elevator decodes the request signals using a specially-designed hardware board. The flow of the elevator entry process is summarized in the following steps: (1) a request signal is sent asking the elevator to come to the current floor and open the door; (2) the processor uses image processing techniques to determine whether the elevator door is open or not by finding if corners exist in the image; (3) if the elevator door is open, a request signal is sent asking the elevator to stay at the current floor; if not open, the processor goes to Step 1; (4) the previously-mentioned model-based navigation technique is applied to move the ALV into the elevator until the existence of the elevator wall is detected; (5) a request signal is sent asking the elevator to go to the desired floor; (6) a corresponding request signal is sent for lifting up or down; (7) a request signal is sent to close the elevator door.

3. Collision avoidance techniques

An important requirement of ALV functions is the ability to avoid obstacles during navigation sessions. In order to avoid obstacles, the ALV must first have the ability to detect them. In this study, photoelectric sensors are employed to detect obstacles. A photoelectric sensor emits a constant beam; meanwhile, it senses whether the beam is reflected. If a reflected beam is received, it means that there is an obstacle at a certain distance from the sensor. In this case, the ALV will stop, and wait until the obstacle disappears, before proceeding. If the obstacle is the elevator door, the ALV will perform the elevator entering process.

As mentioned previously, three photoelectric sensors are used in this study. When guiding the ALV to navigate in the building corridor, the upper photoelectric sensor is utilized to detect front obstacles (e.g., human beings) at a long distance. The sensor is sensitive to obstacles no more than 75 cm away. When coming close to the elevator door, the ALV disables the sensing function of the upper photoelectric sensor and enables the sensing function of the right photoelectric sensor to detect the existence of the elevator door. The sensor is sensitive to obstacles within a range of approximately 30 cm. The third photoelectric sensor is used to detect the wall of the elevator for collision avoidance at a short distance. The sensor is sensitive to obstacles within a range of approximately 15 cm.

ALV LOCATION TECHNIQUE

In the proposed approach, corners and baseline segments are utilized for ALV location. The 3-D locations of corners and baseline segments are inferred from 2-D images through camera calibration and inverse perspective transformation. It is supposed that camera calibration results have already been obtained, and that the height of each baseline of the walls is known in advance. Therefore, only one camera need be used, and the difficult image correspondence problem can be avoided. The ALV location process includes finding the 3-D corner coordinates with respect to the ALV, using DWC-based matching to obtain the ALV position, and computing the slopes of baseline segments to obtain the slant angle of the ALV. The details are described in the following sections.

1. Guidance by model matching

The global coordinates of the corners detected from each input image can be calculated according to the estimated ALV locations (described later). Since the

estimated ALV location is not very accurate due to control errors, the global coordinates of the detect corners are not accurate, either. Proposed in this study is a method that matches each of these detected corners against the model to get the accurate coordinates of these corners.

More specifically, let the input corners constitute an input pattern, which we denote as a point set $S=\{s_1, s_2, \ldots, s_n\}$, where each point s_i denotes a corner. Within a reasonable distance tolerance range, a model pattern M can be extracted from the entire navigation environment. The distance tolerance range can be determined according to the inaccuracy of the mechanical devices. Now, consider any point s_i in S. The points in the model that are possible to match s_i form a subset of M, which we denote by $M_i=\{m_{i1}, m_{i2}, \ldots, m_{ik}\}$. The points in M_i are those points that are within the area of a circle whose center is s_i and the radius is the distance tolerance.

The employed method determines which point in M_i matches s_i in the following way: for any point m_{ij} in M_i, shift all of the points in S so that s_i is superimposed on m_{ij}, and estimate the correlation between S and M using a correlation measure. If superimposition of s_i on m_{ij} gets the maximal correlation measure value, we say that s_i and m_{ij} is the best match pair. The position coordinates of m_{ij} are then used to replace those of s_i.

The distance-weighted correlation (DWC) proposed by Fan and Tsai [4] is employed as our correlation measure. A brief review of the DWC is as follows.

M and S are two point-type patterns to be matched in a two-dimensional space. After M and S are registered and overlapped, the minimum distance d_i of a point s_i in S is defined to be the distance between s_i and its closest point m_{ij} in M. And the weight $W_i(K)$ of a point s_i in S is defined to be

$$W_i(K) = \begin{cases} 1/(d_i^2 + 1) \text{ if } 0 \leq d_i \leq K, \\ 0 \qquad \text{otherwise,} \end{cases} \tag{1}$$

where K is a constant that defines a distance limit within which the closest feature point m_{ij} in M of s_i is searched for.

The DWC value between M and S is defined as

$$C(M, S) = \sum_{i \in S} W_i(K)/N_s, \tag{2}$$

where N_s is the total number of feature points in S.

An example of DWC-based matching is shown in Fig. 3. An image obtained by the camera is shown in Fig. 3a. Three corners are detected in the image, and are shown in Fig. 3b. Note that only corners are drawn with small circles. Within an error range, the input pattern and the model pattern are superimposed as shown in Fig. 3c. The possible match pairs are shown in Fig. 3d. Note that each point in the input pattern is assigned to a point set in the model pattern. The result of matching is shown in Fig. 3e. Each point in the input pattern is now assigned to a single point in the model pattern.

2. Coordinate systems and transformations

Four coordinate systems and relevant coordinate transformations are reviewed here for use in the following sections. The coordinate systems are shown in Fig. 4. The image coordinate system (ICS), denoted as u-w, is attached to the image plane and the u-w plane coincides with the image plane. The camera coordinate system (CCS), denoted as u-v-w, is attached to the camera lens center. The vehicle coordinate system (VCS), denoted as x-y-z, is attached to the contact point of a front wheel

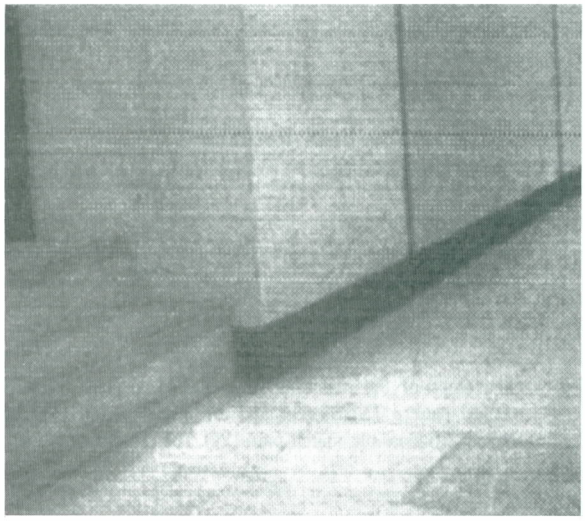

(a)

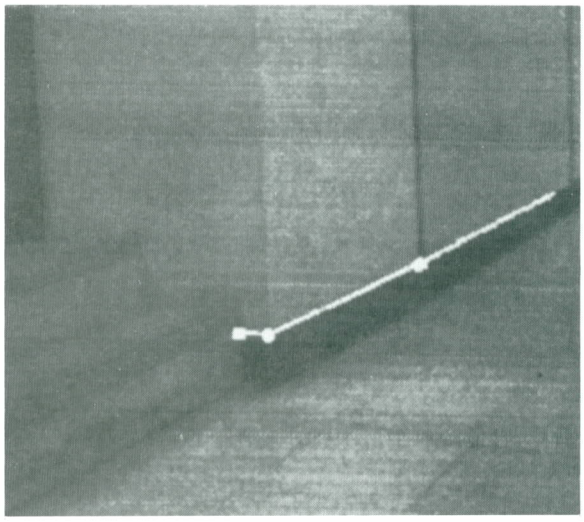

(b)

Fig. 3. The steps of the matching procedure. (a) An input image. (b) Three corners are detected.

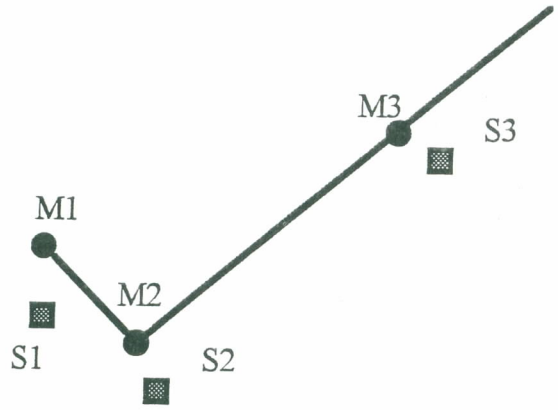

(c)

possible match pairs:

point in sensed pattern	points in model pattern
S1	{M1,M2}
S2	{M1,M2}
S3	{M3}

(d)

result of matching:

point in sensed pattern	point in model pattern
S1	M1
S2	M2
S3	M3

Fig. 3. The steps of the matching procedure(continued). (c) The sensed pattern {S1,S2,S3} and the model pattern{M1,M2, M3}. (d) Possible match pairs. (e) The matching result.

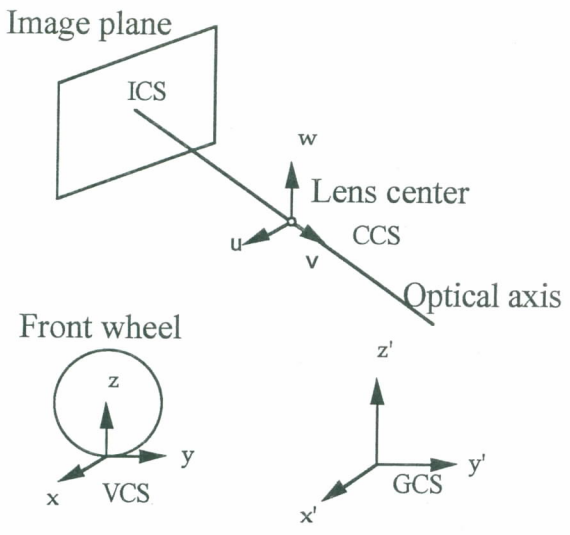

Fig. 4. The camera coordinate system $u-v-w$, the vehicle coordinate system $x-y-z$, and the global coordinate system $x'-y'-z'$.

of the vehicle and the ground. The x-axis and the y-axis are placed on the ground and are parallel to the short and long sides of the vehicel body, respectively. The global coordinate system (GCS), denoted as x'-y'-z', is located at a certain corner in the corridor. The x'-axis and y'-axis are defined to lie on the ground.

The GCS is assumed to be fixed all the time, while the VCS is moving with the vehicle during navigation. The location of the vehicle can be ascertained once the relation between the VCS and the GCS is found. Since the vehicle is on the ground at all time, the z-axis and the z'-axis can be ignored.

The transformation between the CCS and the VCS can be written in terms of homogeneous coordinates[5] as

$$(u\ v\ w\ 1) = (x\ y\ z\ 1)\begin{bmatrix} 1 & 0 & 0 & 0 \\ 0 & 1 & 0 & 0 \\ 0 & 0 & 1 & 0 \\ -x_d & -y_d & -z_d & 1 \end{bmatrix}\begin{bmatrix} r_{11} & r_{12} & r_{13} & 0 \\ r_{21} & r_{22} & r_{23} & 0 \\ r_{31} & r_{32} & r_{33} & 0 \\ 0 & 0 & 0 & 1 \end{bmatrix} \quad (3)$$

where

$$\begin{aligned} r_{11} &= \cos\theta\cos\psi + \sin\theta\sin\phi\sin\psi, \\ r_{12} &= -\sin\theta\cos\phi, \\ r_{13} &= \sin\theta\sin\phi\cos\psi - \cos\theta\sin\psi, \\ r_{21} &= \sin\theta\cos\psi - \cos\theta\sin\phi\sin\psi, \\ r_{22} &= \cos\theta\cos\phi, \\ r_{23} &= -\cos\theta\sin\phi\cos\psi - \sin\theta\sin\psi, \\ r_{31} &= \cos\phi\sin\psi, \\ r_{32} &= \sin\phi, \\ r_{33} &= \cos\phi\cos\psi, \end{aligned} \quad (4)$$

and θ is the pan angle, ϕ the tilt angle, ψ the swing angle, of the camera with respect to the VCS; (x_d, y_d, z_d) is the translation vector from the origin of the CCS to the origin of the VCS.

The transformation between the two 2-D coordinate systems $x-y$ and $x'-x'$ can be written as follows:

$$(x'\ y'\ 1) = (x\ y\ 1)\cdot$$

$$\begin{bmatrix} \cos\omega & \sin\psi & 0 \\ -\sin\psi & \cos\psi & 0 \\ 0 & 0 & 1 \end{bmatrix} \begin{bmatrix} 1 & 0 & 0 \\ 0 & 1 & 0 \\ x'_p & y'_p & 1 \end{bmatrix} \quad (5)$$

where (x'_p, y'_p) is the translation vector from the origin of $x'-y'$ to the origin of $x-y$ and ψ is the relative rotation angle of $x-y$ with respect to $x'-y'$, as shown in Fig. 5. The vector (x'_p, y'_p) and the angle ψ determine the position and the direction of the vehicle in the GCS, respectively.

In practice, the formula for calculating the VCS coordinates of a corner point on a baseline is derived in the following way. As shown in Fig. 6, after backprojecting the point P in the image into the VCS, we can get a line L which passes the lens center and P. The intersection point of this line L and the horizontal plane going through the baseline is the corresponding space point of P, which is the point desired. Denote this point as P'.

The equation of the horizontal plane can be set

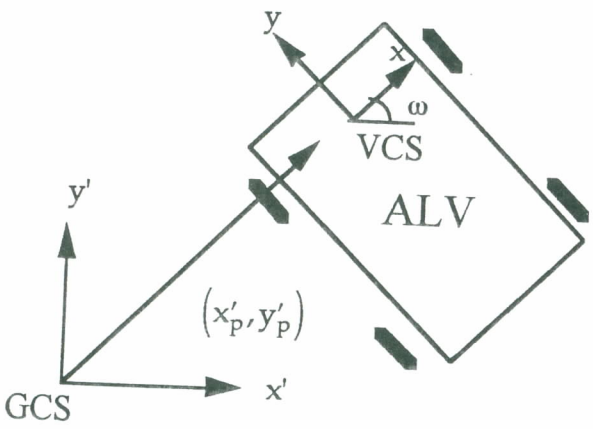

Fig. 5. The relation between 2-D coordinate system $x-y$ and $x'-y'$ represented by a translation vector (x'_p, y'_p) and a relation angle ψ.

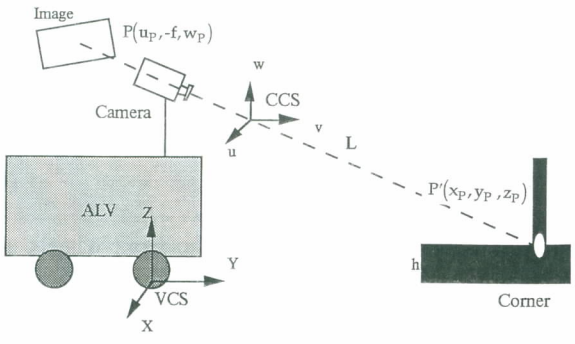

Fig. 6. Configuration of the system for finding the back-projection point for an image pixel.

to be $z=h$ by measuring height h of the baseline of the wall before navigation. Assume that point P in the image has the coordinates $(u_P, -f, w_P)$ in the CCS where (u_P, w_P) indicates its position in the image and f is the focal length. Using Eq. (3), we get the VCS coordinates (x_P, y_P, z_P) of point P in the image as

$$x_P = u_P(\cos\theta\cos\psi + \sin\theta\sin\phi\sin\psi) + f(\sin\theta\cos\phi) + w_P(\sin\theta\sin\phi\cos\psi - \cos\theta\sin\psi) + x_d,$$

$$y_P = u_P(\sin\theta\cos\psi - \cos\theta\sin\phi\sin\psi) - f(\cos\theta\cos\phi) - w_P(\cos\theta\sin\phi\cos\psi + \sin\theta\sin\psi) + y_d,$$

$$z_P = u_P(\cos\phi\sin\psi) - f\sin\phi + w_P(\cos\phi\cos\psi) + z_d,$$

where (x_d, y_d, z_d) are the coordinates of the lens center in the VCS. On the other hand, the equation of line L is

$$\frac{x - x_d}{x_P - x_d} = \frac{y - y_d}{y_P - y_d} = \frac{z - z_d}{z_P - z_d} = k. \quad (6)$$

Since point P' is a corner point on line L, by substituting $z=h$ into Eq. (6), the desired VCS coordinates (x'_P, y'_P, z'_P) of point P' can be solved to be:

$$x_{P'} = x_d + \frac{h - z_d}{z_P - z_d}(x_P - x_d),$$

$$y_{P'} = y_P + \frac{h - z_d}{z_P - z_d}(y_P - y_d),$$

$$z_{P'} = h. \quad (7)$$

3. Determination of ALV slant angle

As mentioned previously, the ALV location is described by the ALV slant angle ψ and the ALV position (x'_p, y'_p). To derive the ALV location in the GCS, we rewrite Eq. (5) as follows:

$$x' = x\cos\psi - y\sin\psi + x'_p$$

$$y' = x\sin\psi + y\cos\psi + y'_p. \quad (8)$$

In our approach, the ALV slant angle ψ is solved first, and the ALV position (x'_p, y'_p) is solved accordingly.

After a corner P_C detected from the input image is matched with the model, the baseline segment L which intersects P_C is used to determine the slant angle of the ALV. If more than one corner is detected from the input image, only the corner with the maximal DWC value (which is obtained in the matching steps) is used. Both the slope of this baseline segment in the VCS coor-

dinate system and that in the GCS coordinate system are computed.

The slope of baseline segment L in the VCS is determined by selecting any two points, say P_1 and P_2, in L. Because all points in a baseline segment are located on the wall, the VCS coordinates of P_1 and P_2 can be determined using Eq. (7). More specifically, assume that the VCS coordinates of P_1 and P_2 are computed to be (x_1, y_1) and (x_2, y_2) (ignore the z coordinates), then the slope m_1 of baseline segment L in the VCS can be computed by

$$m_1 = \frac{y_1 - y_2}{x_1 - x_2} .$$

In determining the slope of the baseline segment in the GCS, it is assumed that any two consecutive corners in the mode are located on an identical plane. This is reasonable because almost all of the surfaces of the walls or doors in a building are planes, and corners are always found on the boundaries of these planes. Under this assumption, only two GCS points that lie on a baseline segment need be found to compute the slope of the baseline segment in the GCS. The first GCS point P_1' is the corner in the model correspponding to P_C. The second GCS point P_2' is selected to be the corner point in the model next to P_1' with P_1' and P_2' forming the baseline segment L' in the model corresponding to L mentioned previously.

Because the GCS coordinates of P_1' and P_2' have been stored in the model, the GCS coordinates of these two points can be determined. Assume that the GCS coordinates of the two points are (x_1', y_1') and (x_2', y_2') (ignore the z' coordinates), then the slope m_2 of the baseline segment L' in the GCS can be computed to be

$$m_2 = \frac{y_1' - y_2'}{x_1' - x_2'} .$$

After the slopes of the baseline segment in the VCS and in the GCS are determined, the slant angle of the ALV can be derived. This is illustrated in Fig. 7.

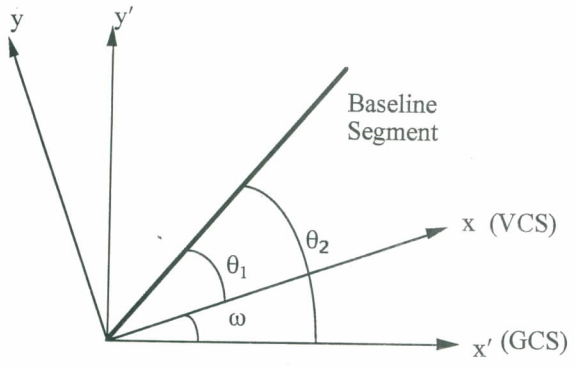

Fig. 7. The slopes of baseline segment in the GCS and in the VSC are used to solve the slant angle of ALV.

The angle θ_1 between the baseline segment and the positive x-axis of the VCS, and the angle θ_2 between the baseline segment and the positive x'-axis of the GCS can be derived to be

$$\theta_1 = \tan^{-1} m_1,$$

$$\theta_2 = \tan^{-1} m_2.$$

Finally, the slant angle ψ of the ALV can be solved to be

$$\psi = \theta_2 - \theta_1 .$$

4. Determination of ALV global position

The position of a detected corner in the VCS and in the GCS are used to determine the ALV position. Note that the VCS coordinates (x, y) of the corner can be determined as discussed in Sec. 3.2. After matching with the model as discussed in Sec. 3.1, the GCS coordinates (x', y') of the corner are also determined. Also, the ALV slant angle ψ has been solved, as mentioned above. By substituting ψ, (x, y), and (x', y') into Eq. (8), the position of the ALV can be determined to be

$$x_p' = x' - x\cos\psi + y\sin\psi,$$

$$y_p' = y' - y\sin\psi - y\cos\psi .$$

5. Modification of ALV location result

The ALV moves forward for a certain distance during the time interval from the instant of obtaining an image to completing the calculation of the ALV position. So, the measured ALV location should be recomputed after this time duration. As shown in Fig. 8, let the vehicle be located at A originally. After moving a distance S forward during the time interval, let the vehicle be at a new location B. What we desire to know is the relative location of B with respect to A, denoted by a vector $\boldsymbol{T}$, given the distance S (computed as the product of the vehicle speed and the time duration). By basic kinematics of the ALV, the rotation radius R can be found to be

$$R = \frac{d}{\sin\delta} \qquad (9)$$

where d is the distance between the front wheels and the rear wheels, and δ is the turn angle of the front wheels. The angle γ can be determined as

$$\gamma = \frac{S}{R} . \qquad (10)$$

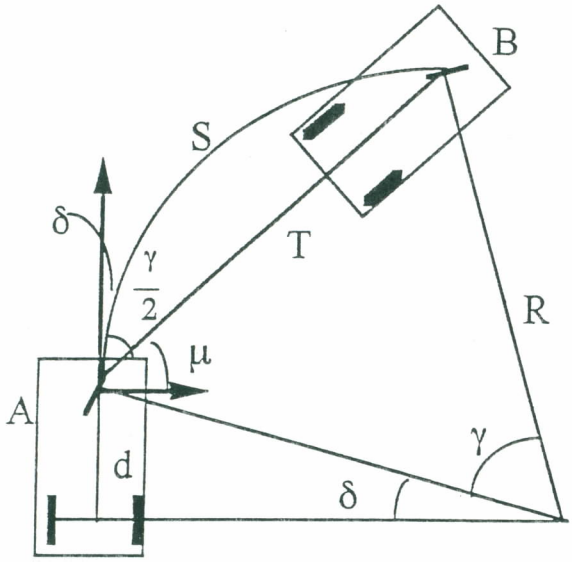

Fig. 8. The vehicle locations before and after the ALV moves a distant S forward.

So, the length of vector $\boldsymbol{T}$ can be solved to be

$$T_i = R\sqrt{2(1 - \cos\gamma)}$$

and the direction of vector $\boldsymbol{T}$ is

$$\mu = \frac{\pi}{2} - \delta - \frac{\gamma}{2} .$$

The VCS coordinates of location B with respect to location A can thus be computed by

$$x = T_i \cos\mu ,$$

$$y = T_i \sin\mu .$$

After the front wheel location of the ALV is determined, the rear wheel location (b_x, b_y) of the ALV can also be determined to be

$$b_x = x + d \sin\gamma ,$$

$$b_y = y - d \cos\gamma .$$

6. Determination of ALV wheel turn angle

A method for computing the ALV front wheel turn angle δ was proposed by Cheng and Tsai [2] and is employed by this study. A brief review of the method is as follows. Given a reasonable moving distance S and the turn angle of the ALV front wheels, the locations of the front wheels and the rear wheels can be determined as discussed in Section 3.5. Given a straight path P, define $E_P^F(\delta)$ to be the distance from the front wheels of the ALV to the given path P after the ALV traverses a distance S with the turn angle δ. So the value of D_P^F is determined by the turn angle δ. Similarly, define $D_P^B(\delta)$ as the distance from the rear wheels of the ALV to the given path P after the ALV traverses a distance S with the turn angle δ. The value of D_P^B is also determined by the turn angle δ.

A closeness measure $L_p(\delta)$ of the ALV to the given path is then defined to be

$$L_p(\delta) = \frac{1}{1 + D_P^F(\delta) + D_P^B(\delta)} . \qquad (11)$$

A larger value of L_p means that the ALV is closer to the path P. It is easy to verify that $0 < L_p \leq 1$, and that $L_p = 1$ if and only if both of the front wheels and both of the rear wheels of the ALV are located right on the path.

EXPERIMENTAL RESULTS

A series of ALV navigation experiments were conducted in a building corridor and an elevator in National Chiao Tung University. Forty-four corners in the environment are stored and used for our experiments. A preselected path for the ALV to follow is illustrated in Fig. 9. The model (corner positions) and the environment contour are also shown in the figure for reference. Each corner is marked by a small black spot. The navigation path is approximately 40 m in length. Each experimental navigation session starts from a corner of the corridor, and involves driving through a right-turn corner of the corridor, driving to the elevator, and entering the elevator. The navigation speed of the vehicle is about 25 cm/sec in a straight corridor section and 15 cm/sec at a turning area. About 170 to 200 navigation cycles are performed in a complete navigation session. The computation time of a navigation cycle ranges approximately from 1.6 to 2.8 seconds for different images.

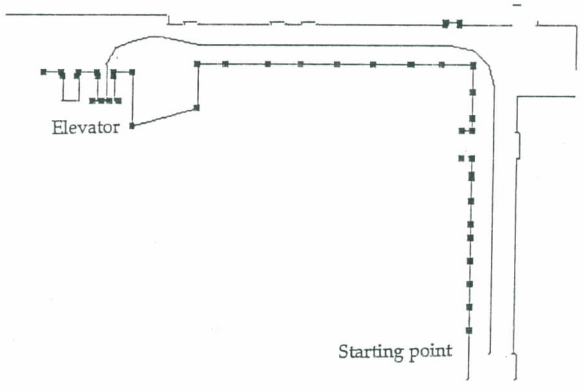

Fig. 9. The path for the ALV navigation, and the positions of corners (marked by black squares).

Several successful navigation sessions have been performed. In Fig. 10 two separate navigation sessions, (I) and (II) respectively, are traced. Each block square in the figure represents a vehicle location which is obtained from the matching process of a navigation cycle.

Sometimes erroneous corners may be produced or certain corners may be missed after input images are preprocessed. However, our experiments have shown that in most cases, due to the use of the model matching technique for ALV guidance one or two erroneous or missing corners will not affect the matching results. Even when the matching result is poor, causing the ALV to navigate unsmoothly, the ALV will come back to its predetermined path in the next several cycles.

CONCLUSIONS AND SUGGESTIONS

An integrated approach for ALV navigation and collision avoidance in building corridors and elevators has been proposed by fusing computer vision, radio, and photoelectric sensing techniques. Several successful navigation sessions in real time confirm the effectiveness of this approach. The main contributions of this study are as follows: First, a computer vision approach is proposed to locate an ALV by the use of multiple house corners. The locations of corners in the navigation environment are stored as models in advance, so extension of the model is easy and only a little storage space is required. Second, the combination of the techniques of radio control and model-base guidance has been proved to be a feasible method for guiding the ALV to enter an elevator automatically. Finally, an obstacle avoidance approach which utilizes photoelectric sensors for ALV navigation is developed.

There are several ways in which the proposed ALV guidance method may be improved. First, more flexible guidance schemes to absorb control errors due to the mechanical structure inaccuracy of the ALV should be designed. Second, more sophisticated methods to achieve complete between-floor transportation are desired. Finally, it would be beneficial to further investigate the possibility of equipping the ALV guidance system to automatically learn environments and to automatically construct environmental models.

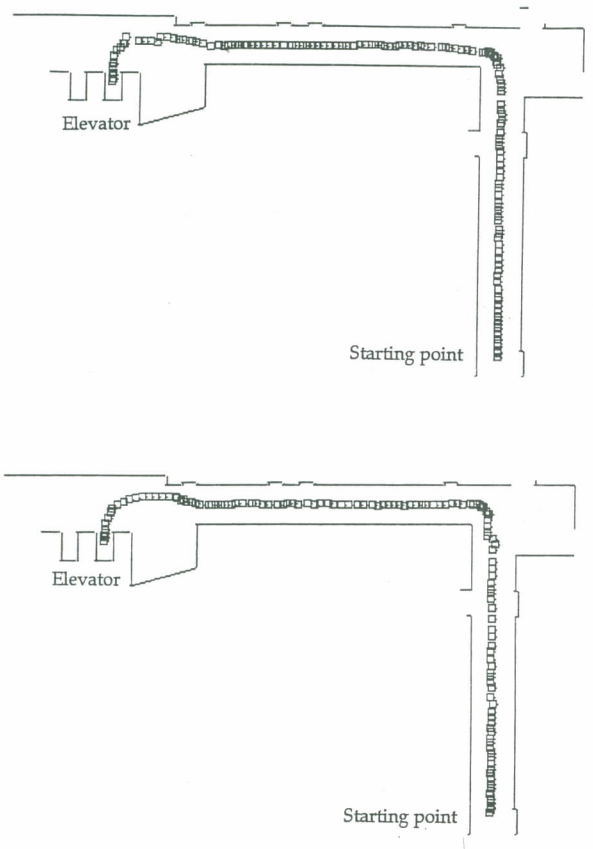

Fig. 10. Examples of traces of navigation sessions. (a) Session I. (b) Session II.

ACKNOWLEDGEMENT

This work was supported partially by the National Science Council, Republic of China under Grant NSC81-0404-E009-010.

REFFERENCES

1. Chatila, R. and J. Laumond, "Position Referencing and Consistent World Modeling for Mobil Robots," in *Proc. IEEE Int. Conf. on Robotics and Automation,* St. Louis, MO, U.S.A., pp. 138-145 (1985).
2. Cheng, S.D. and W.H. Tsai, "Model-based Guidance of Autonomous Land Vehicles in Indoor Environments by Structured Light Using Vertical Line Information," *Journal of Electrical Engineering*, Vol. 34, No. 6, pp. 441-452 (1991).
3. Cox, I.J., "Blanche: An Autonomous Robot Vehicle for Structured Environments," in *Proc. IEEE Int. Conf. on Robtics and Automation*, Philadelphia, Pa., U.S.A., pp. 978-982 (1988).
4. Fan, T.J. and W.H. Tsai, "Automatic Chinese Seal Identification," *Computer Vision, Graphics and Image Processing,* pp. 311-330 (1984).
5. Foley, J.D. and A.V. Dam, *Fundamentals of Interactive Computer Graphics*, Addison-Wesley, Reading, MA, U.S.A. (1982).
6. Ke, W.J. and W.H. Tsai, "Indoor Autonomous Land Vehicle Guidance by Corner Tracking Using Computer Vision," in *Proceedings of Workshop on Computer Vision, Graphics and Image Processing,* Tainan, Taiwan, Republic of China, pp. 133-139, Aug. (1991).
7. Madarasz, R.L., L.C. Heiny, R.F. Cromp and H.M. Mazur, "The Design of an Autonomous Land Vehicle for the Disabled," *IEEE J. Rob. Autom.* Vol.

RA-2, pp. 117-126, Sept. (1986).

Discussions of this paper may appear in the discussion section of a future issue. All discussions should be submitted to the Editor-in-Chief.

Manuscript Received: Aug. 5, 1992
Revision Received: Oct. 27, 1992
and Accepted: Nov. 19, 1992